Experimental progress towards the MicroThrust MEMS electrospray electric propulsion system

IEPC-2013-146

Presented at the 33rd International Electric Propulsion Conference,
The George Washington University • Washington, D.C. • USA
October 6 – 10, 2013

C. Ryan[1], A. Daykin-Iliopoulos[2], and J. Stark[3]
Queen Mary University of London, London, E1 4NS, United Kingdom

A. Z. Salaverri[4], E. Vargas[5], and P. Rangsten[6]
SSC NanoSpace, Uppsala Science Park, SE-751 83, Uppsala, Sweden

S. Dandavino[7], C. Ataman[8], S. Chakraborty[9], D. Courtney[10] and H. Shea[11]
École Polytechnique Fédérale de Lausanne (EPFL), Neuchatel, 2000, Switzerland

Abstract: This paper describes the experimental progress towards an operational microfabricated electrospray thruster, as part of the EU FP7 "MicroThrust" Project. Microfabrication of an electrospray multiplexed thruster allows the seamless manufacturing of arrays of emitters, combining high specific impulse with sizeable thrust. The resulting thruster can thus be extremely efficient with a thrust approaching ≈100μN, depending on array size. We are working within the European FP7 project MicroThrust consortium to develop the complete MEMS electrospray array thruster for 10-100 kg class satellites to enable these small spacecraft to perform large delta-V missions (5 km/s). This includes the manufacture of MEMS Silicon electrospray emitters, and also a passive propellant feeding system, a miniaturized high voltage power supply, and the investigation of possible missions. We report here on the experimental testing of the micromachined Silicon capillary arrays, constituting arrays of either 91 or 127 emitters. A detailed description of the manufacture of the arrays will be described in a separate companion paper. To increase the specific impulse and thrust, and to reduce the plume angle, an accelerator has been integrated into the thruster Silicon chips. The thrust, and specific impulse has been measured using a Time-of-Flight (ToF) system, whilst the emitter current has been measured as the applied voltage was varied. The plume angle has been discerned using a translating Faraday cup.

[1] Post-doc, School of Engineering and Materials Science, Queen Mary University of London, c.n.ryan@qmul.ac.uk
[2] Masters student, School of Engineering and Materials Science, Queen Mary University of London, a.j.n.daykin-iliopoulos@se10.qmul.ac.uk
[3] Professor, Queen Mary University of London, j.p.w.stark@qmul.ac.uk
[4] Development engineer, SSC NanoSpace, Uppsala, Sweden, ana.salaverri@sscspace.com
[5] Development engineer, SSC NanoSpace, Uppsala, Sweden, Ernesto.Vargas@sscspace.com
[6] Vice President Engineering, SSC NanoSpace, Uppsala, Sweden, pelle.rangsten@sscspace.com
[7] PhD Student, Ecole Polytechnique Fédérale de Lausanne (EPFL), simon.dandavino@epfl.ch
[8] Group leader, IMTEK, Germany, caglar.ataman@imtek.uni-freiburg.de
[9] PhD Student, Ecole Polytechnique Fédérale de Lausanne (EPFL), Switzerland, subha.chakraborty@epfl.ch
[10] Post-doc, Ecole Polytechnique Fédérale de Lausanne (EPFL), Switzerland, daniel.courtney@epfl.ch
[11] Associate Professor, Ecole Polytechnique Fédérale de Lausanne (EPFL), Switzerland, herbert.shea@epfl.ch

Nomenclature

BB	=	BreadBoard (model)
EIFB	=	Electrical Interface Board
EMI-BF_4	=	1- Ethyl-3-Methylimidazolium Tetrafluoroborate
EMI-SCN	=	1- Ethyl-3-Methylimidazolium Thiocyanate
EPDM	=	ethylene propylene diene monomer rubber
HLOW	=	BB model Housing Lower
HUPP	=	BB model Housing Upper
HVPS	=	High Voltage Power Supply
IL	=	Ionic Liquid
I_{sp}	=	Specific Impulse
PCB	=	Printed Circuit Board
PCS	=	Power and Control System
PEEK	=	Polyether Ether Ketone
PFIC	=	Propellant Feeding Interface Chip
PIR	=	Purely Ionic Regime
QMUL	=	Queen Mary University of London
RPA	=	Retarding-Potential-Analysis
T	=	Thrust
THC	=	Thruster chips (microfabricated thruster arrays)
ToF	=	Time of Flight
TRL	=	Technology Readiness Level

I. Introduction

With their small size and low power consumption microfabricated electrospray ion sources offer a promising propulsion technology for small (<100 kg) spacecraft. Electrospray emitters operate by transporting a propellant, typically an ionic liquid, to the tip of an emitter. This fluid transport can occur due to wicking in the case of an externally wetted [1, 2] and porous emitters [3, 4], or by an external pressure source and/or wicking for a capillary-like emitter[5-8].

By the application of a potential difference between the emitter and an opposing electrode a strong electric field is created. This field forces the liquid into a Taylor cone [9], with charged droplets emitted from the cone-jet tip when using a liquid like Ethylene Glycol. If though an ionic liquid (IL) is used as a propellant, it has been found that the electric field is sufficiently intense (due to the ionic liquids high surface tension and conductivity[10]) to result in a spray of both ions and droplets. In some cases a Purely Ionic Regime (PIR) occurs, with no droplets present within the plume[11]. This results in a specific impulse of several thousand seconds, although combined with a strong reduction in emitter thrust.

The MicroThrust Project is using the capillary emitter electrospray technique, with an ionic liquid as the propellant. The emitters are microfabricated using Silicon etching processes, which offer good manufacturing precision at the micron level. In the design of the final system the propellant is not pressure-driven, being fed from the propellant chamber using the capillarity forces. This offers greater simplicity than a pressure fed propellant flow system.

Currently the MicroThrust consortium is working towards a BreadBoard (BB) model which is broadly representative, and demonstrates some systems needed, for a working thruster system. This includes a BB model system which is fairly representative of a thruster system, including bipolar spraying, a Power and Control System (PCS), and large arrays of microfabricated emitters. These emitters have been successfully operated, with the spray current as a function of voltage (referred to herein as the IV characteristic) plume angle characteristics, and the Time of Flight (ToF) measurements investigated.

This work is carried out in the framework of the MicroThrust project which aims to develop to Technology Readiness Level (TRL-5) a system based on this technology.

II. Microfabricated thrusters, holders, and experimental setup

A. Microfabricated thrusters

The process of microfabrication of the thruster 'chips' (THCs) is described in detail in a companion paper[12]. The thruster consists of an emitter Silicon wafer and an extractor-accelerator silicon-glass wafer sandwiching a 50 µm thick polymer layer. A cross section of this assembly is shown in Figure 2. Within the emitter wafer the capillaries stand off the silicon surface by 80 µm. Each capillary has an individual extractor electrode with a suitably sized orifice. The extractor-accelerator wafer consists of a glass wafer through which are micro-sandblasted apertures. Aluminium is then coated on the top surface to form the accelerator, and a silicon extractor is anodically bonded to the bottom side. The extractor, once bonded to the glass, is then machined away until it is 50 µm thick. The glass layer itself is 250 µm thick.

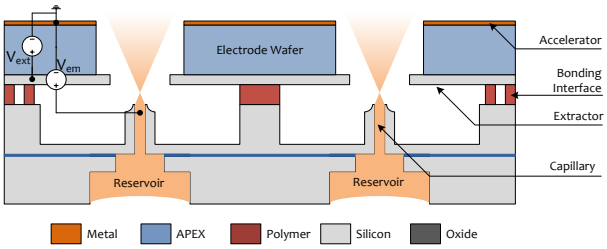

Figure 2. Schematic of breadboard thruster design cross-section.

These processes result in a chip which is 15mm square and approximately 1mm thick (Figure 1). Access to the extractor and accelerator is via diagonally opposing contact points, with two for each grid (the accelerator and extractor grids) to allow for diagnostic testing of connections.

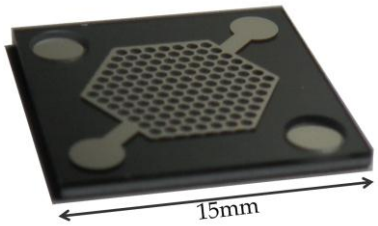

Figure 1. Image of a large electrospray array.

Two types of emitter array have been manufactured having either 91 or 127 emitters. The accelerator aperture differs for the two types of arrays, with a bigger 800µm aperture for the 91 emitter array, whilst the 127 emitter array accelerators have an 550µm aperture. The extractor aperture is 168 µm for both arrays.

B. Holders for experimental testing

Two holders were available for testing of the manufactured thruster chips: a "simple breadboard (BB) holder", and a more complex full BB model.

Figure 3. Simple BB holder, with and without thruster chip present.

1. Simple BB holder

A simple holder was manufactured from Polyether Ether Ketone (PEEK), with a central Aluminium section (Figure 3). The central Aluminium section makes connection to propellant. The chip sits on an O-ring within an indentation in the Aluminium section. A simple PCB with four pogo (spring loaded) pins makes contact with the extractor and accelerator contact points on the front side of the chip, and also compresses it into the O-ring. Electrical connection for both the extractor and accelerator is made on the backside of the holder to the four bolts which also provide the compression.

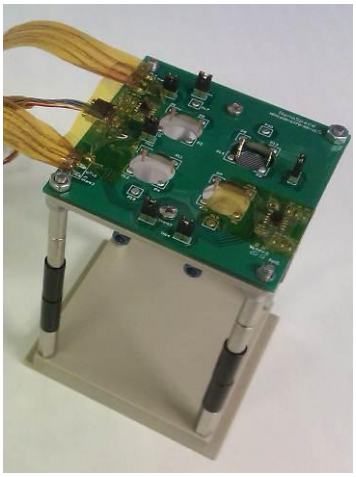

Figure 4. Full (complex) BB holder.

2. BB model

The MicroThrust full BB model is illustrated in Figure 4. The BB model was manufactured by SSC NanoSpace, Sweden. It consists of;

- A lower housing (HLOW) to contain the propellant and form the lower interface with the thruster chip, manufactured from transparent acrylic to allow the amount of propellant to be seen. The thruster chip sits on an EPDM O-ring inserted into an

indentation in the HLOW. Note that the HLOW has four separate propellant chambers, allowing for the spraying of four thruster chips simultaneously.

- An upper housing (HUPP) manufactured from PEEK used to compress the thruster chip onto the O-ring contained within the HLOW.
- An electrical interface board (EIFB) PCB making the electrical connections to the thruster chips. Contact to the thruster chips was again through pogo pins. Six high voltage wires carry the necessary thruster voltages, with two being 'emitter' voltages (two pairs of thruster chips share the same emitter voltages), and four extractor voltages. The ground (for the accelerator) is carried by an Omnetics © connector, along with connections for two temperature sensors located on the top surface of the EIFB.
- The thruster chips themselves are glued onto 'interface' chips, using Ellesworth Adhesives 3M Scotch Weld 2216 B/A epoxy. Currently the interface chip consists of 21*21mm by 0.9mm thick square stainless steel pieces with a slight indentation for the thruster chip to sit in, and a large 12.5mm hole to allow for the propellant to access the backside of the thruster chips. At a later stage of thruster development this interface chip will be replaced by a 'Propellant Feeding Interface Chip' (PFIC), which will be similar but with individual propellant feeding channels to the backside of each of the emitters, forming a part of an overall propellant wicking system for the electrospray thruster system.

The BB model is mounted on four Aluminium rods connected to a PEEK base with two L-shaped grooves. These grooves slide into a suitable mount situated within the vacuum chamber.

The BB model also includes a vacuum compatible Power & Control System (PCS), designed by SystematIC Design b.v. Details of the PCS are provided in a separate paper[13]. This provides a bipolar voltage of ±3000V to the emitter, and up to 1000V below this voltage to the extractor. It is designed to be mounted onto the four rods that form the base of the BB model (see Figure 4). The PCS is though under development so experiments described herein use desktop High Voltage Power Supplies (HVPS's) supplied by FuG Ltd.

C. Experimental set-up

The experimental set-up is similar to that described previously[14].

For the calculation of the thrust and specific impulse, time-of-flight (ToF) measurements are used, as illustrated in Figure 5. The test bench consists of a 400mm diameter by 400mm long cylindrical vacuum chamber. This chamber has a smaller 6-way cross chamber of 200mm diameter attached to its top to allow for easy insertion of the test set-up. A smaller separate chamber is used as a propellant reservoir, connected to the main chamber by fused silica tubing. The base pressure attained in the main chamber is 1×10^{-6} - 1×10^{-5} mbar and in the fluid reservoir ~1.3×10^{-3} mbar. The thruster chips are connected to commercial power supplies, with separate supplies to each of the emitter and extractor. The electrospray currents on the emitter, extractor and accelerator are measured by three potential divider systems, measuring the voltage drops across 100kΩ high power resistors. The three voltmeters are connected to the PC via optically isolated cables, allowing for data logging of current on the emitter, extractor and accelerator.

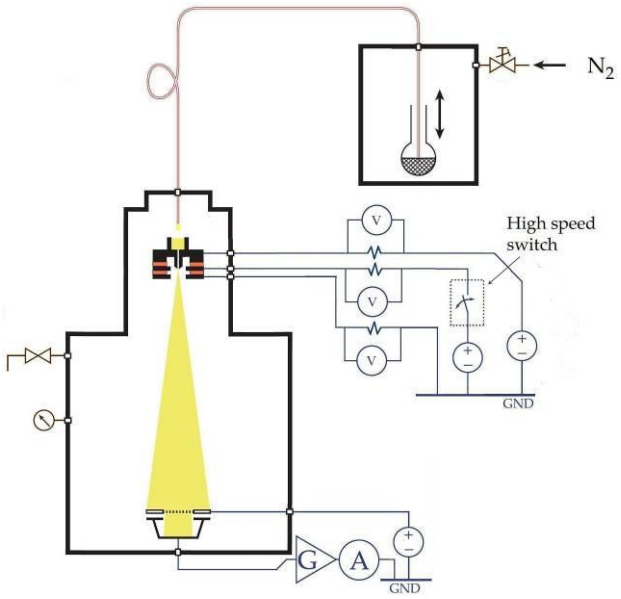

Figure 5. QMUL Time-of-Flight vacuum chamber system for current emitter testing.

For time-of-flight measurements, rather than using a simple electrostatic gate downstream as used previously[14], a DEI PVX-4150 high speed switch is attached to the extractor, with the output of the switch being either ~900V below the emitter voltage (for spraying to occur), or switched to the emitter voltage to stop the spraying within the switch speed of 20 nanoseconds, resulting in a Time-of flight trace downstream. This ToF method has been applied before to electrospray devices[6].

The thruster plume is collected on a 220mm diameter flat plate situated up to 500mm downstream. The current collected is amplified by a Femto variable-gain high-speed current amplifier. The signal is then supplied to a Wavesurfer oscilloscope for analysis and collection. A fine mesh is situated above the plate, to which is applied a negative potential difference to suppress secondary electron emission.

Alternatively a vacuum compatible translation stage can be used downstream, allowing for the translation of a Faraday cup or other devices across the plume. The stage can translate a distance of 280mm, and is illustrated in Figure 6. It was specially commissioned for this project.

Not illustrated in Figure 5 is a high voltage bipolar relay switch capable of changing the emitter voltage polarity at a frequency of up to 10Hz. This allows for bipolar spraying, an addition that has been found necessary to avoid electrochemical degradation occurring on the emitter conductive surface[15]. In this configuration both the extractor and accelerator are grounded.

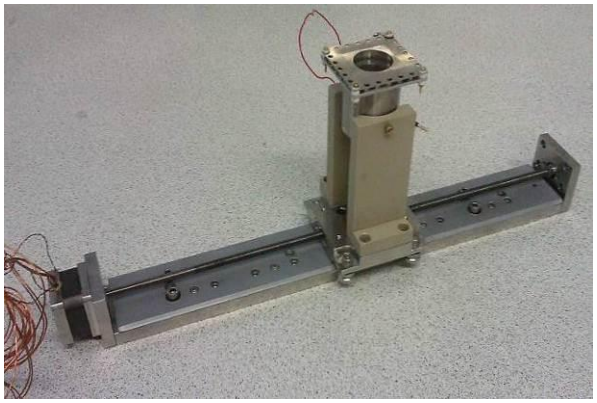

Figure 6. Vacuum compatible motorized translation stage, with Faraday cup attached.

D. Experimental method

The thruster assembly (either the simple thruster holder or the more complex BB model) is inserted vertically pointing downwards into the main chamber, and the chamber is pumped down to below 10^{-5}mBar. Once base pressure is reached, propellant (typically EMI BF_4) is fed from the small reservoir chamber, and droplet fed using gravity into the backside of the thruster chip. Using this method, rather than having the propellant reservoir directly attached to the thruster assembly, has been found to reduce the likelihood of the liquid over-pressurisation short circuiting the emitter and extractor[16]. The liquid wicks through to the emitter tip, using capillary action. In a flight-ready thruster, a fully integrated propellant feed system is necessary, using capillary action. The development of this feeding system is ongoing.

Once the liquid has wicked through to the emitter tip the applied voltage is increased on the emitter, and the experimental run is begun.

III. Experimental Results

E. Current-voltage measurements

Figure 7 plots the emitter current, measured at the emitter using the potential divider system, against the applied voltage difference between the emitters and the extractor. The emitted current is proportional to the plume current. Data is plotted for various 'acceleration' voltages, V_{accn}, defined as the voltage applied to the extractor to raise it above ground. The actual accelerator on the THC is at ground throughout. Data is also shown for the two versions of the THC: the 127 emitter and 91 emitter array.

There is a strong linear trend of emitter current that would seem independent of the acceleration voltage or the THC type. The independence of the current to the acceleration voltage demonstrates that the electric field within the emitter-extractor region is not affected by field conditions downstream, and so the plume can be accelerated without affecting the emission process.

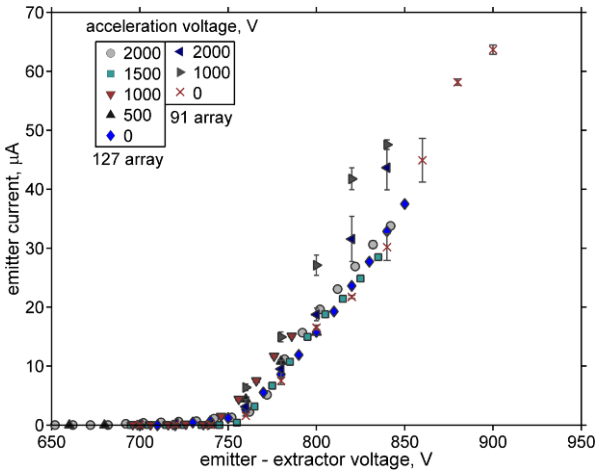

Figure 7. Variation of emitter current with voltage difference between emitter and extractor, at different acceleration voltages.

The gradient of the IV relationship in Figure 7 is ~0.4μA per emitter-extractor volt. This strong relationship is in agreement with previous studies[17].

The independence of the emitter current trend to the THC type is unexpected, with a larger current expected from the larger 127 emitter THC array. An explanation is the small gravitational pressure head from the 10mm of propellant within the holder may be dominating over the capillary pressure. If so, this is evidence that a complete propellant feeding (i.e. wicking) system is needed. These are though initial results, with further testing needed to fully confirm this lack of dependence on emitter number.

There is also some suggestion that the 91 emitter array is less stable, with the IV curves of this THC demonstrating more variation than the 127 emitter array, especially so when an acceleration voltage is applied.

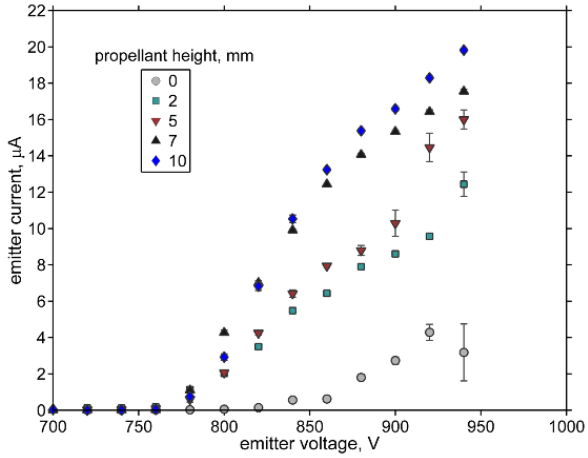

Figure 8. Variation of emitter current with emitter voltage, at different propellant heights.

To investigate the effect of the gravitational pressure head height, an emitter array was put into the simple holder, and then the holder was filled with EMI-BF4 propellant. Spray was then initiated; fluid was then removed from the holder reservoir region, although fluid was retained within the emitter due to the high surface tension forces arising from the small emitter diameter. With the reservoir emptied, spray was attempted using only the fluid within the emitter chip itself; this is the data described in Figure 8 with 0mm of propellant height. The holder was then incrementally filled, with at each increment an IV sweep completed. The resulting data shows the IV gradient increasing as the propellant holder is filled to its maximum of 10mm. This suggests that the gravitational head height is having an effect, and the filling process is not entirely due to propellant wicking through the emitters.

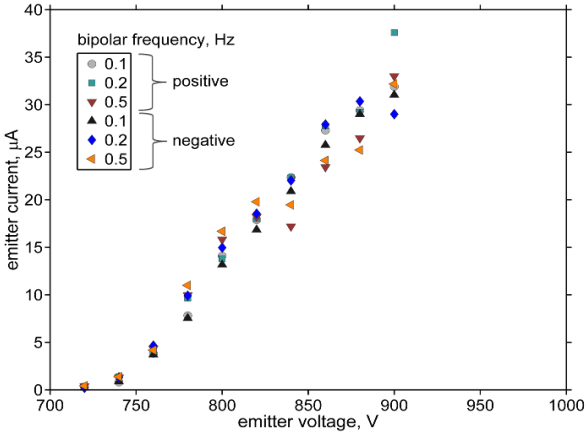

Figure 9. Variation of emitter current with emitter voltage, at different bipolar frequencies.

Bipolar IV data using an array has also been collected, as shown in Figure 9. This was completed using a bipolar switch manufactured at QMUL, similar to one used before[7]. Data is shown for three different frequencies, in both negative and positive mode. Higher frequency data was also collected, but the 2Hz logging frequency of emitter current data was insufficient to capture faithfully the current changes. Analysis of downstream current data collected through the high speed amplifier is currently underway. From the results presented in Figure 9 it appears that there is little effect on the IV trend with switching frequency, or polarity, suggesting that charge balancing maybe of less concern, at least over short time periods.

F. Time-of-Flight (ToF) measurements

Figure 10 illustrates ToF data for EMI-BF_4 collected as described in Section II C. Results are shown for differing acceleration voltages, with the voltage difference between emitter and extractor being +900V. The plume is dominated by ions, but with a small proportion of droplets present, as demonstrated by the long tail of the ToF traces. The collected current increases as the acceleration voltage increases; this is a demonstration of the plume becoming more focused. The large collector plate does not capture the full plume until the plume is focused by the acceleration voltage.

The specific impulse and the thrust can be calculated using the integral equations typically applied;

$$I_{sp} = \frac{L_{TOF}}{2\, g_0} \frac{\int_0^\infty i(t)\mathrm{d}t}{\int_0^\infty i(t)\, t\, \mathrm{d}t} \tag{1}$$

where g_0 is earth's gravitational constant, L_{TOF} the distance between the ToF gate and the collector plate. The thrust can also be calculated from the ToF trace;

$$T = \frac{2V}{L} \int_0^\infty I(t)dt \tag{2}$$

Where V is the voltage accelerating the charged particles (assumed to be the applied emitter voltage).

Figure 11 illustrates the calculated total thrust from the array and the specific impulse, as the acceleration voltage is increased. Both the specific impulse I_{sp} and thrust increase, with the voltage reaching 1000s, and the thrust 7μN.

Since the MicroThrust Project has the overall aim to produce a breadboard thruster which has the performance to make a mission to near planets or other Near Earth Objects feasible using a small spacecraft, the achieved specific impulse should be of the order of several thousand seconds[18] for the required ΔV. In order to achieve this target complete removal of the droplet component of the spray is required. This can be achieved by reducing the flow rate by further increasing the hydraulic impedance; indeed our group has demonstrated the Purely Ionic Regime using EMI-BF_4 in a 19 emitter array filled with microbeads[8]. The emitters described here though do not have microbeads within their inner diameter, as the process of depositing the microbeads has proved unreliable. The alternative approach, adopted by the MicroThrust group is to manufacture emitters with small enough inner diameters that would approach the hydraulic impedance that one could expect from a bead filled emitter. Calculations demonstrate that this sized emitter should be 5μm[14]. Due to microfabrication delays this small emitter size has not been achieved in the current generation of thruster chips, with the emitter, as described here, having an inner diameter of 10 μm. The new generation of emitters currently in production will however meet this requirement.

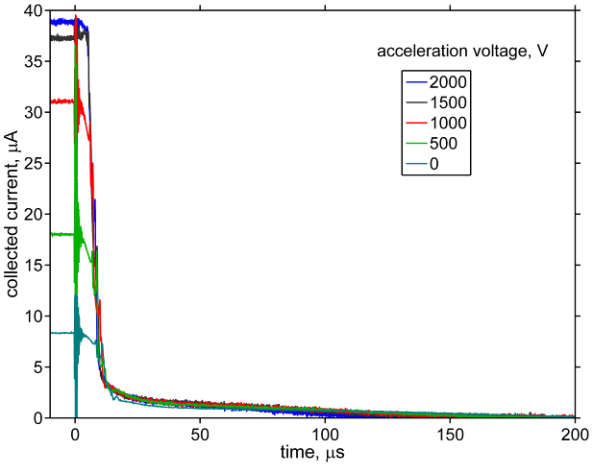

Figure 10. Time-of-flight measurements with an emitter-extractor voltage difference of +900V, at different acceleration voltages.

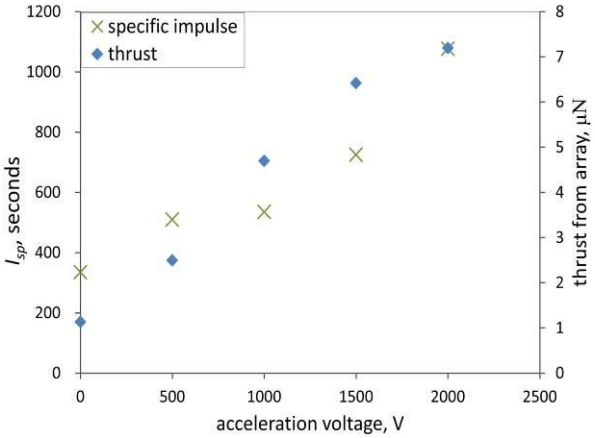

Figure 11. specific impulse and thrust measurements with an emitter-extractor voltage difference of +900V, at different acceleration voltages.

An alternative method to achieve the PIR is to use an alternative ionic liquid. It has been found that ionic liquids with high conductivities and surface tensions can achieve a spray of solely ions without the need for a high hydraulic impedance system [11, 19, 20]. A comprehensive study of novel ionic liquid propellant has been completed as part of the MicroThrust Project, with full results described in an upcoming journal article.

One promising ionic liquid tested is 1- Ethyl-3-Methylimidazolium Thiocyanate, EMI-SCN, with a measured conductivity of 1.85S/m, and a surface tension of 41.9mN/m (measured using a Horiba B-173 conductivity meter and Kruss DSA100 goniometer). Initial tests in a single emitter were carried out and the results demonstrated a purely ionic regime, as illustrated in Figure 13. The testing of the single emitter was similar to that described

previously[14, 21], with the an emitter voltage of +1050V (no accelerator was present). The specific impulse is calculated to be 2700s and the thrust 0.065 µN.

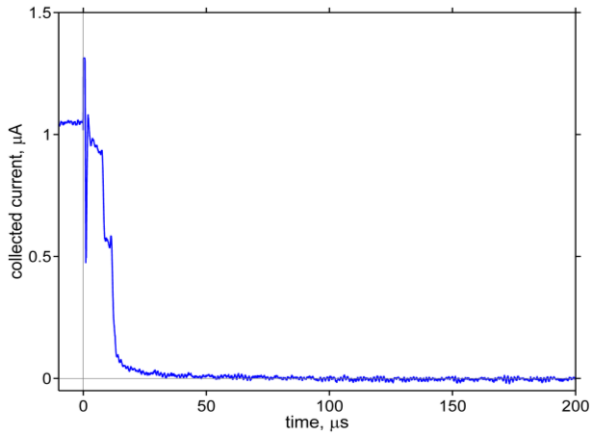

Figure 13. Time-of-flight measurements using EMI SCN in a single emitter.

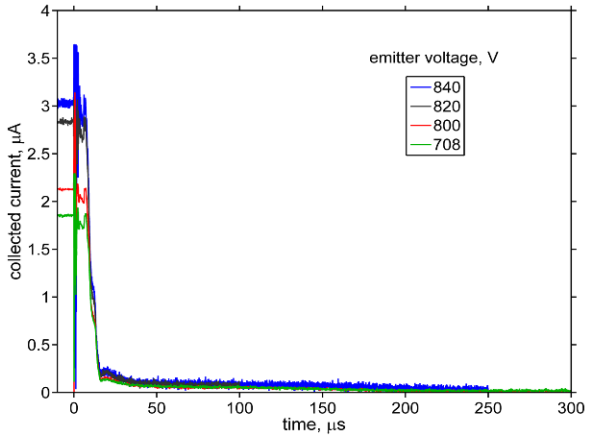

Figure 12. Time-of-flight measurements using EMI SCN in a 127 emitter array.

This potential propellant was then tested in a 127 emitter, with the results illustrated in Figure 12. A very ionic plume was present, although there is a slight hint of a droplet tail. If the droplet tail is present then the specific impulse at 800V is 332, with a thrust of 5.1µN. If there is no droplet tail present then the specific impulse is 3000s, and the thrust ~0.36µN. This great dependence of the specific impulse on whether even 1% of the plume contains droplets has been identified before[22], and is why an increase in hydraulic impedance may be a more reliable method to achieve PIR.

G. Plume angle measurements

The plume half-angle was measured downstream by translating a modified Kimball Physics Faraday cup 280mm across the plume. This spray tests were completed using the BB model (with one THC mounted), with different acceleration voltages applied.

Some preliminary plume profile results are illustrated in Figure 14. Plume focusing is clearly apparent, with a significant change in beam profile as the acceleration voltage is increased.

The plume half angle was calculated from each profile by taking a 10% confidence interval – i.e. integrating the profile up to the angle at which 90% of the profile area is integrated. The results from this are shown in Figure 15.

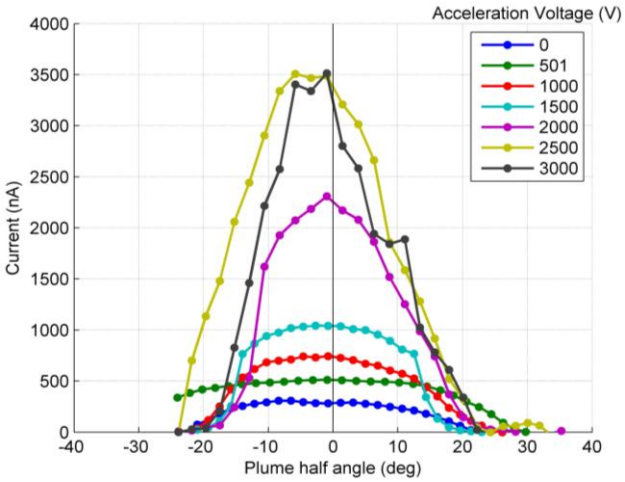

Figure 14. Plume profiles at different acceleration voltages.

The plume is focused, with the angle decreasing from ~25 to 15 degrees. Most of this focusing would seem though to occur within the first 1000V of applied acceleration voltage, and above 1000V little more focusing occurs. The data is relatively scattered, partly due to the sometimes unstable plume, but also due to the data not always being collected at the same voltage difference between the emitter and extractor. As this voltage difference increases the plume half-angle was found to increase.

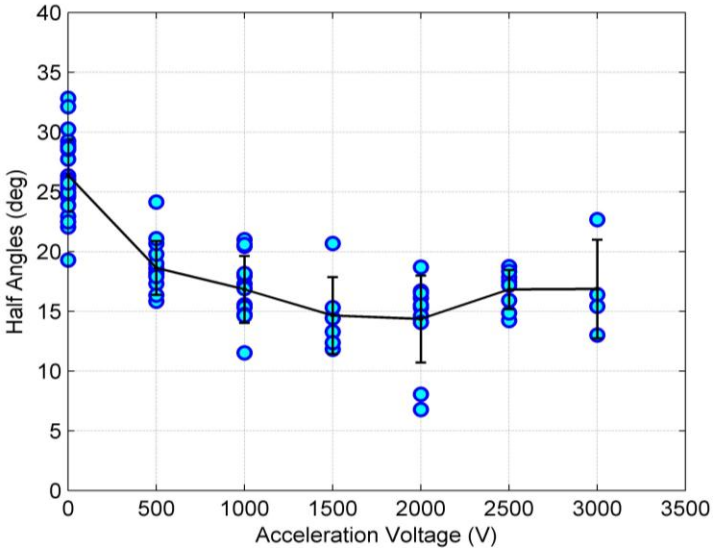

Figure 15. Calculated plume half-angles for different acceleration voltages.

IV. Conclusions

Experimental results have been illustrated that demonstrate the continued improvement of the MicroThrust microfabricated electrospray thruster system. The operation of large arrays of microfabricated Silicon emitters has been demonstrated, both with and without an accelerator present. Time-of-flight data has been collected, including with a novel ionic liquid. Plume angle data has been captured, demonstrating focusing of the plume. Successful operation of the MicroThrust BB model has been shown, demonstrating some improvement in the technology readiness of the thruster. Further improvements have also been identified, which include;

- A fully integrated capillary feeding assembly is needed, to remove the effect of gravity, and to reliable fill all emitters across an array. Work on this has begun, but will not be completed within the MicroThrust Project.
- Reliable PIR operation needs to be demonstrated, with this most likely be obtained through a change in geometry. Emitters with smaller diameters are being manufactured.

Acknowledgments

This work has been partially supported by the MicroThrust project, grant agreement number 263035, funded by the EC Seventh Framework Programme theme FP7-SPACE-2010.

References

1. P. Lozano, B. Glass and M. Martinez-Sanchez, *29th International Electric Propulsion Conference*, Princeton University, 2005, pp. IEPC-2005-2192.
2. P. Lozano and M. Martínez-Sánchez, *Journal of Colloid and Interface Science*, 2005, **282**, 415-421.
3. R. S. Legge and P. Lozano, *Journal of Propulsion and Power*, 2011, **27**, 485-495.
4. D. G. Courtney and P. Lozano, *27th International Symposium on Space Technology and Science,*, Tsukuba, Japan, 2009, pp. ISTS-2009-b-2051.
5. G. Lenguito, J. Fernandez de la Mora and A. Gomez, *46th AIAA/ASME/SAE/ASEE Joint Propulsion Conference & Exhibit*, Nashville, TN, 2010, pp. AIAA 2010-6521.
6. G. Lenguito, J. Fernandez de la Mora and A. Gomez, *47th AIAA/ASME/SAE/ASEE Joint Propulsion Conference & Exhibit*, San Diego, California, 2011, pp. AIAA 2011-5590.
7. R. Krpoun and H. R. Shea, *Journal of Micromechanics and Microengineering*, 2009, **19**, 045019.
8. R. Krpoun, K. L. Smith, J. P. W. Stark and H. R. Shea, *Applied Physics Letters*, 2009, **94**, 163502.

9. G. Taylor, *Proceedings of the Royal Society of London. Series A, Mathematical and Physical Sciences*, 1964, **280**, 383-397.
10. M. Gamero-Castaño and J. Fernández de la Mora, *The Journal of Chemical Physics*, 2000, **113**, 815-832.
11. I. Romero-Sanz, R. Bocanegra, J. F. d. l. Mora and M. Gamero-Castano, *Journal of Applied Physics*, 2003, **94**, 3599-3605.
12. S. Dandavino , C. Ataman, S. Chakraborty, H. Shea, C. Ryan and J. Stark, *33rd International Electric Propulsion Conference*, Washington DC, USA, IEPC-2013-127, 2013.
13. R. Visee, M. de Jong and J. Timmerman, *33rd International Electric Propulsion Conference*, Wasington DC, USA, IEPC-2013-258, 2013.
14. C. Ryan, J. Stark, C. Ataman, S. Dandavino , S. Chakraborty and H. Shea, *AAAF-ESA-CNES Space Propulsion Conference*, Bordeaux, France, 7th – 10th May 2012.
15. P. Lozano and M. Martínez-Sánchez, *Journal of Colloid and Interface Science*, 2004, **280**, 149-154.
16. C. N. Ryan, K. L. Smith, M. S. Alexander and J. P. W. Stark, *Journal of Physics D: Applied Physics*, 2009, **42**, 155504.
17. D. G. Courtney, H. Q. Li and P. Lozano, *Journal of Physics D: Applied Physics*, 2012, **45**, 485203.
18. F. Tata Nardini, M. Straathof, C. Ataman, M. Richard, H. Shea, P. Rangsten, A. Salaverri, C. Ryan, J. P. W. Stark and R. Visee, *AAAF-ESA-CNES Space Propulsion Conference 2012*, Bordeaux, France, 2012.
19. M. Gamero-Castaño and J. F. d. l. Mora, *Journal of Mass Spectrometry*, 2000, **35**, 790-803.
20. D. Garoz, C. Bueno, C. Larriba, S. Castro, I. Romero-Sanz, J. F. d. l. Mora, Y. Yoshida and G. Saito, *Journal of Applied Physics*, 2007, **102**, 064913.
21. S. Dandavino , C. Ataman, S. Chakraborty, H. Shea, C. Ryan and J. Stark, *48th AIAA/ASME/SAE/ASEE Joint Propulsion Conference & Exhibit, AIAA-2012-4024*, Atlanta, Georgia USA, 2012.
22. P. Lozano, PhD, MIT, 2003.